Glycative Stress Research

Online edition : ISSN 2188-3610
Print edition : ISSN 2188-3602
Received : February 3, 2017
Accepted : September 5, 2017
Published online : September 30, 2017

Original article

Glycated-HSA inhibits osteoclastogenesis in RAW264.7 cells depending on the glycating agents via downregulating RANKL-signaling

A. N. M. Mamun-Or-Rashid, Wakako Takabe, Masayuki Yagi, Yoshikazu Yonei

Anti-Aging Medical Research Center and Glycation Stress Research Center,
Graduate School of Life and Medical Sciences, Doshisha University, Kyoto, JAPAN

Abstract

***Background*:** In humans, bone density is reduced with age while advanced glycation endproducts (AGEs) formation and accumulation increases. Therefore, the effect of AGEs on osteoclastogenic differentiation (osteoclastogenesis) or activation is of great importance.

***Methods*:** Murine monocyte/macrophage RAW264.7 cells were cultured in the presence of 100 ng/mL nuclear factor kappa-B ligand (RANKL) for osteoclastogenesis. To prepare AGEs, we used human serum albumin (HSA) with glycating agents (glucose, fructose, glycolaldehyde, glyceraldehyde, glyoxal) and phosphate buffer pH 7.4 incubated at 60 °C for 40 hours and then non-reacted glycating agents and phosphate buffer were removed by ultrafiltration and used in *in vitro* osteoclastogenesis to observe the effects of glycated-HSA. Tartrate resistant acid phosphatase (TRAP) activity was used as an osteoclastogenic marker. Lactate dehydrogenase (LDH) assay was used to check cytotoxicity. A real-time polymerase chain reaction (RT-PCR), western blot analysis was used to check other gene expressions. Calcium influx was measured using a Fluo-8 calcium assay kit.

***Results*:** We found glycated HSA inhibited RANKL-induced osteoclastogenesis in RAW264.7 cells depending on the glycating agents and fluorescent AGEs used. Secreted high mobility group box protein1 (HMGB1) is known to bind with receptors for AGEs (RAGE) and play an important role in osteoclastogenesis. We found that glycolaldehyde and glyceraldehyde derived glycated-HSA inhibited RANKL-induced HMGB1 secretion, downregulate osteoclastogenic nuclear factor-κB (NFκB), nuclear factor of activated T-cells cytoplasmic 1 (NFATc1), c-Fos, calcium influx without altering RAGE expression.

***Conclusion*:** This study indicated that glycation of HSA plays a significant role in bone turnover.

***KEY WORDS*:** osteoclastogenesis, RANKL (receptor activator of nuclear factor kappa-B ligand), glycation, advanced glycation endproducts, HMGB1 (high-mobility group box 1)

Introduction

Advanced glycation endproducts (AGEs) are chemical modifications of proteins or lipids by carbohydrates or the degradation products of carbohydrates formed by a non-enzymatic unavoidable reaction known as the maillard reaction. As they lose their native structure, they cause several autoimmune diseases, mainly by activating receptors for AGEs (RAGE), followed by inflammatory osteoclastogenic cytokine tumor necrosis factor alpha (TNFα), interleukin 1 beta (IL-1β), and interleukin 6 (IL-6) secretion. Pentosidine levels in bone collagen, serum and urine increase with age. The age-related AGE increase in bone and serum is a phenomenon observed in both men and women. The amount of AGEs formation and accumulation is positively correlated with age, whereas bone forming osteoblast cell differentiation correlates negatively [1-5]. Elevated level of AGEs in both male and female osteoporosis patients also demonstrated the link between AGEs and bone loss, and therefore fracture risk [6-8].

Bone is made of inorganic metal crystals, an organic extracellular matrix, mainly type I collagen, lipids, water, bone forming cell osteoblast, osteocytes (trapped osteoblast in the osteoid), lining cells and bone resorbing cell osteoclasts. Bone remodeling is a lifelong process of bone resorption

Corresponding author: Wakako Takabe, PhD
Anti-Aging Medical Research Center and Glycative Stress Research Center,
Graduate School of Life and Medical Sciences, Doshisha University
1-3 Tatara Miyakodani, Kyotanabe, Kyoto 610-0394, Japan
TEL& FAX: +81-774-65-6382 Email: wtakabe@mail.doshisha.ac.jp
Co-authors: Mamun-Or-Rashid ANM, mamunbtgeiu@gmail.com ;
Yagi M, myagi@mail.doshisha.ac.jp ; Yonei Y, yyonei@mail.doshisha.ac.jp

and rebuilding by the bone cells that originated and are differentiated from osteogenic stem cells [9-11]. Therefore, the differentiation, maturation, and activation of these cells are of great importance in bone development. Bone mechanical behavior, morphology changed and became weaker with age in men and women, resulting in increased risk of bone fracture [8, 12, 13]. The amount of AGE formation and bone weakening are positively correlated with age and both of the bone cells possess RAGE [14], therefore, there could be alteration in the regulation of bone remodeling by the AGEs.

Osteoclasts are giant multinucleated cells, originated from hematopoietic cells, which resorb the bone matrix and activate osteoblast cells to rebuild the bone. Osteoclastogenesis is regulated solely by receptor activator of nuclear factor kappa-B ligand (RANKL) that is secreted by osteoblast cells. RAGE on osteoclast precursor cell surface plays a crucial role by binding with extracellular high-mobility group box 1 (HMGB1) and activating related downstream signaling to differentiate into mature osteoclast cells [14]. As, RAGE also binds with AGEs and triggers inflammatory cytokine production, we investigated if there any direct effect of glycated-HSA on osteoclastogenesis. We used different glycating agents to prepare HSA-AGEs and found that they have an inhibitory effect on differentiation, based on the glycating agents, without causing cell death.

Materials and methods

Cell culture and reagents

Murine monocyte/macrophage RAW264.7 (ATCC® TIB-71TM) cell line was purchased from American Type Culture Collection (ATCC; Manassas, VA). Cells were grown in Dulbecco's modified Eagle's medium (DMEM; Sigma-Aldrich, St. Louis, MO) supplemented with 10% fetal bovine serum (FBS; Nichirei Biosciences, Tokyo, Japan), penicillin 100 units/mL, streptomycin 100 µg/mL and amphotericin B 25 µg/mL (Gibco, El Paso, TX) at 37 °C under the condition of 5% CO_2 [15, 16]. Passages three to six were used for all experiments.

Glycated-HSA preparation

To prepare glycated-HSA, we used 8 mg/mL HSA along with several glycating agents, 0.2 M glucose (Glu) or fructose (Fru), or 33 mM glycolaldehyde (Glycol) or glyceraldehyde (Glycer) or Glyoxal (GO) in 0.05 M phosphate buffer (pH 7.4) and incubated at 60 °C for 40 hours [17]. In the case of heated-HSA, we used milliQ instead of glycating agents. After that, we removed the remaining unreacted glycating agents and phosphate buffer using Amicon ultra-4 10K (Millipore, Darmstadt, Germany) centrifugal devices according to the manufacturer's instruction. Briefly, 4 mL of protein mixture was placed into the centrifugal devices and centrifuged at 7500 ×g for 15 minutes. Then washed using sterile milliQ and centrifuged again to collect heated or glycated proteins. The amount of protein was measured using a BCA protein assay (Thermo Scientific, Rockford, IL).

Measurement of fluorescent AGEs

Purified protein samples (AGEs or heated) 150 µg/mL were used to measure fluorescence intensity. A quinine sulfate solution was used as a reference for the calibration of fluorescent materials and the fluorescence intensity was measured at 370/440 nm using a Varioscan® Flash (Thermo Scientific, Waltham, MA) microplate reader [17, 18].

In vitro osteoclastogenesis

RAW264.7 cells were seeded in multi-well plates and incubated for 24 hours for cell attachment. Then, media were changed with αMEM (Gibco) with the previously mentioned concentration of native, heated or glycated-HSA, 100 ng/mL recombinant mouse RANK Ligand (rmRANKL, R&D Systems, Minneapolis, MN) with FBS and antibiotics [19]. After three days, medium was renewed. After five days of cultures, cells were observed by multiple assays as mentioned.

TRAP activity

RAW264.7 cells treated with the previously mentioned proteins were fixed after five days of treatment using a cell fixation buffer (acetone : ethanol = 1 : 1) and then fixed cells were used to measure TRAP activity with a TRAP solution kit (Oriental Yeast Co., Tokyo, Japan) according to the manufacturer's instructions. Colorimetric absorbance were taken at 405 nm using a Varioscan® Flash microplate reader [19].

Evaluation of glycated proteins on cell viability and proliferation

To check cytotoxic cell death and cell proliferation, a lactate dehydrogenase (LDH) assay and WST-8 assay was performed as previously described [16]. After five days of treatment with the indicated substances, cells were used for the WST-8 assay and cultured media from each well was used for the LDH release assay, respectively. After incubating with an assay solution and red color development, colorimetric absorbance was measured at either 490 nm (LDH) or 450 nm (WST-8) using a Varioscan® Flash microplate reader.

Isolation of total RNA and RT-PCR

RAW264.7 cells were seeded into 24-well plates at a density of 4×10^4 cells/well and incubated for 24 hours. Then, the media were changed and incubated under the previously mentioned time and conditions. After that, total RNA was extracted using Isogen II reagent (Nippon Gene, Tokyo, Japan) according to the manufacturer's instructions. Five-hundred ng total RNA was reverse-transcribed with PrimeScript™ RT Master Mix (Takara Bio Inc., Shiga, Japan) using Applied Biosystems 2720 Thermal cycler (Thermo Fisher Scientific, Waltham, MA).

RT-PCR was performed with a Thunderbird™ SYBR qPCR mix (Toyobo Co., Osaka, Japan) according to manufacturer's instructions [16] with gene-specific primers (Invitrogen, Tokyo, Japan). The primers used are as follows: Integrin β3, 5′-TTA CCC CGT GGA CAT CTA CTA-3′ (forward), 5′-AGT CTT CCA TCC AGG GCA ATA-3′ (reverse) [14]; Traf6, 5′-GAA GAG GTC ATG GAC GCC AA-3′ (forward), 5′-CGG GTA GAG ACT TCA CAG CG-3′ (reverse); Dcstamp, 5′-TCC TCC ATG AAC AAA CAG TTC CAA-3′ (forward), 5′-AGA CGT GGT TTA GGA ATG CAG CTC-3′ (reverse); Ocstamp, 5′-ATG AGG ACC ATC AGG GCA GCC ACG-3′ (forward), 5′-GGA GAA GCT GGG TCA GTA GTT CGT-3′ (reverse) [20]; NFATc1, 5′-GGA GCG GAG AAA CTT TGC G-3′ (forward), 5′-GTG ACA CTA GGG GAC ACA TAA CT-3′ (reverse); c-Fos,

5′-CGG GTT TCA ACG CCG ACT A-3′ (forward), 5′-TTG GCA CTA GAG ACG GAC AGA-3′ (reverse); Matrix metallopeptidase 9 (MMP-9), 5′-CTG GAC AGC CAG ACA CTA AAG-3′ (forward), 5′-CTC GCG GCA AGT CTT CAG AG-3′ (reverse); Cathepsin K, 5′-GAA GAA GAC TCA CCA GAA GCA G-3′ (forward), 5′-TCC AGG TTA TGG GCA GAG ATT-3′ (reverse); Glyceraldehyde 3-phosphate dehydrogenase (GAPDH), 5′-AGG TCG GTG TGA ACG GAT TTG-3′ (forward), 5′-TGT AGA CCA TGT AGT TGA GGT CA-3′ (reverse) [21]; TRAP, 5′-GCG ACC ATT GTT AGC CAC ATA CG-3′ (forward), 5′-CGT TGA TGT CGC ACA GAG GGA T-3′ (reverse); ATPase H+ Transporting V0 Subunit D2 (Atp6v0d2), 5′-ACG GTG ATG TCA CAG CAG ACG T-3′ (forward), 5′-CCT CTG GAT AGA GCC TGC CGC A-3′ (reverse) [22]; TNFα, 5′- ACC CTC ACA CTC AGA TCA TCT TC-3′ (forward), 5′- TGG TGG TTT GCT ACG ACG T-3′ (reverse); IL-1β, 5′-TGT AAT GAA AGA CGG CAC ACC-3′ (forward), 5′-TCT TCT TTG GGT ATT GCT TGG-3′ (reverse); IL-6, 5′-ACA ACC ACG GCC TTC CCT ACT T-3′ (forward), 5′-CAC GAT TTC CCA GAG AAC ATG TG-3′ (reverse); RAGE, 5′-ACT ACC GAG TCC GAG TCT ACC-3′ (forward), 5′-GTA GCT TCC CTC AGA CAC ACA-3′ (reverse) [16]. GAPDH was used as an internal control. To determine the effect of NFκB pathway on gene expression, BAY11-7082 (Cayman Chemical, Ann Arbor, MI) was used.

Protein Extraction and Western Blot Analysis

RAW264.7 cells were seeded in 6-well plate at a density of 2×10^5 cells/well and incubated for 24 hours. Then, they were treated with αMEM supplemented with 10% FBS, antibiotics and the previously mentioned concentration of RANKL with or without glycated or heated-HSA for the indicated time periods, and then cells were lysed with RIPA buffer containing 50 mM Tris-HCl, 150 mM NaCl, 0.1% SDS, 1% Triton ×-100 with complete protease inhibitor (Wako Pure Chemical Industries, Osaka, Japan) and phosphatase inhibitor (Roche Applied Science, Penzberg, Germany). Cell lysates were electrophoresed by sodium dodecyl sulfate polyacrylamide gel electrophoresis (SDS-PAGE) (10% polyacrylamide), then proteins were transferred on a polyvinylidene difluoride (PVDF) membrane followed by blocking with a 5% skim milk solution in TBS-T. Then, the membranes were immunoblotted with each primary antibody. The antibodies against GAPDH, RAGE and HMGB1 were from Abcam (Cambridge, UK), and the remaining antibodies were from Cell Signaling Technology (Danvers, MA). The antigen–antibody complexes were visualized with the appropriate secondary antibodies (Santa Cruz Biotechnology, Dallas, TX) and chemiluminescence horseradish peroxidase (HRP) substrate along with detection system as recommended by the manufacturer. The results illustrated in each figure are representative of three independent experiments. ImageJ was used to measure the optical density of the protein bands.

SiRNA experiments

For siRNA treatment, we used lipofectamine RNAiMAX transfection reagent (Thermo Fisher Scientific) as per manufacturer's protocol and allowed growth for three days. To determine HMGB1 protein, which react by HMGB1 antibody and showed several bands, we used small interfering RNA against HMGB1 (siHMGB1 #s205520, Thermo Fisher Scientific) to transfect RAW264.7 cells. Then cell lysate and media were western blotted to observe HMGB1 production and secretion. To observe the effects of RAGE, we used siRAGE (#162189, Thermo Fisher Scientific) to transfect the cell. Then, the cells were treated as mentioned in the figures.

Nuclear and Cytoplasmic protein extraction

A nuclear and cytoplasmic extraction reagent kit (Thermo Fisher Scientific) was used to fractionate nuclear and cytoplasmic proteins as per manufacturer's instructions. Then, protein lysate was used along with a protease inhibitor. A phosphorylase inhibitor was used to observe protein expression or phosphorylation by western blot.

Measurement of intracellular calcium mobilization:

The effects of glycated-HSA on RANKL-stimulated calcium mobilization were measured using a Fluo-8 no wash calcium assay kit (Abcam) according to the manufacturer's instructions. Fluorescence intensity was measured at Excitation/emission (Ex/Em) = 490/525 nm using a Varioscan® Flash microplate reader.

Statistical analysis

Data were expressed as mean ± standard error of the mean (SEM). All statistical analyses were performed using a Tukey-Kramer test for intergroup comparison in all of the experiments. Differences were considered significant at a significance level of 5%.

Results

Fluorescence intensity of glycated-HSA.

Glycation produces fluorescent AGEs [17, 18], so we checked the fluorescence intensity of 150 μg/mL glycated-HSA. Fluorescence intensity was significantly increased depending on the glycating agents. Glucose-derived glycated-HSA (HSA-Glu) showed lowest and glycolaldehyde-derived glycated-HSA (HSA-Glycol) showed highest fluorescence intensity (***Fig. 1-A***).

Glycolaldehyde and glyceraldehyde-derived glycated-HSA inhibited osteoclastic differentiation of RAW264.7 cells.

HSA is one of the major proteins that are present in high amounts in blood circulation, and thereby present in the bone microenvironment. Therefore, we investigated the effect of glycation of HSA on RANKL-induced osteoclastogenesis in RAW264.7 cells. We used native, heated or glycated HSA in the presence of 100 ng/mL RANKL for five days. Then TRAP activity was measured. As shown in ***Fig. 1-B***, native, heated, HSA-Glu and fructose-derived glycated-HSA (HSA-Fru) have no effect on TRAP activity, whereas HSA-Glycol, glyceraldehyde-derived glycated-HSA (HSA-Glycer) and glyoxal-derived glycated-HSA (HSA-GO) significantly reduced TRAP activity. Because LDH release was not observed under this condition, HSA-Glycol, HSA-Glycer and HSA-GO inhibited TRAP activity without inducing cell death (***Fig. 1-C***). We further checked the effect of HSA-Glycol and HSA-Glycer on cell morphology and cell

proliferation. We found that HSA-Glycol and HSA-Glycer decreased the number and size of multinucleated osteoclast cells (***Fig. 1-D***) and induced cell proliferation (***Fig. 1-E***) compared with RANKL treatment alone. Native and heated HSA did not affect cell numbers. These data indicate that HSA-Glycol and HSA-Glycer inhibited the differentiation in osteoclasts.

To investigate the time point which glycated-HSA affect on osteoclastogenesis, we further evaluated TRAP activity of RANKL-treated RAW264.7 cells at five days with glycated proteins for all five days (Total), first three days (day 0 to 3, Early) and later two days (day 3 to 5, Late). In our experimental results, when cells were cultured with HSA-AGEs for the first three days then washed them out, RANKL-induced TRAP activity at five days was not altered (***Fig. 1-F***, Early), while the later two days of treatment of HSA-AGEs reduced TRAP activity as same as a five-day treatment (***Fig. 1-F***, Late and Total). Glycated-HSA did not induce TRAP activity in the absence of RANKL.

We also performed RT-PCR analyses to investigate the effect of HSA-AGEs on osteoclastogenic gene expression. Early osteoclastogenic and fusion related markers like TRAF-6, integrin β3, DC stamp, OC stamp, none of the glycated-HSA showed any effect until 3 days treatment (***Fig. 2-A***). In the case of osteoclastic maturation and activation marker gene expression, we found TRAP, CTSK, MMP9 mRNA expression were inhibited by HSA-Glycol and HSA-Glycer, whereas, Atp6v and the receptor for AGEs (RAGE) mRNA expression remained unchanged (***Fig. 2-B***).

Glycated-HSA inhibited osteoclastogenic cytokine production.

Glycated-HSA is also known for inducing osteoclastogenic and inflammatory cytokine production in macrophage cells [15, 16], so next we checked whether HSA-Glycol and HSA-Glycer stimulate inflammatory mRNA expression in osteoclastogenic culture medium or not. We found that TNFα mRNA expression was reduced at 150 μg/mL, but significantly increased at higher concentration, 500 μg/mL, whereas, IL-1β, IL-6 mRNA expression was significantly reduced by glycated-HSA (***Fig. 2-C***). By all means, HSA-Glycol and HSA-Glycer inhibited RANKL-induced osteoclastogenesis in RAW264.7 cells.

HMGB1 expression and secretion in the experimental conditions.

HMGB1 is a multifunctional nuclear protein that interacts with nucleosomes, transcription factors, and histones in the nucleus. However, when it is secreted, it binds with inflammatory receptor RAGE and plays a vital role in cytokine production and in osteoclastogenesis [14]. Therefore, we investigated the effect of glycated-HSA on HMGB1 expression and secretion and RAGE expression in the RAW264.7 cells. First, we treated RAW264.7 cells with RANKL at different time points to observe its effects on HMGB1 expression and secretion along with RAGE. In cell lysate we found that HMGB1 expression remained unchanged, but RAGE expression was induced by RANKL treatment for 18 hours to three days, then declined (***Fig. 3-A***). HMGB1 secretion was observed after 36 hours and reached its peak after three days of treatment. On day 4, it declined, as we had to replace the media after three days. HMGB1 secretion was highest after three days, so we choose three days of incubation for the remainder of the experiments. HMGB1 antibody shows three different bands, so next we verified whether all are HMGB1 or not by using siHMGB1 transfection experiments. SiHMGB1 less changed those three bands in cell lysate, while the secreted proteins were downregulated (***Fig. 3-B***).

Then, we checked the effects of heated and glycated-HSA on HMGB1 expression and secretion and RAGE expression by RAW264.7 cells. HMGB1 and RAGE expression in cell lysate were not changed by glycated-HSA (***Fig. 3C***), however, HMGB1 secretion was reduced (***Fig. 3-D***). Next, we checked whether HMGB1 secretion is inhibited by glycated proteins in a dose dependent manner. We checked 150 and 500 μg/mL of glycated-HSA, both of them reduced HMGB1 (25 kDa) secretion, but increased 17 kDa by HSA-Glycol (***Fig. 3-E***).

HMGB1 translocation from nucleus to cytoplasm also changed by glycated-HSA.

As HMGB1 is a nuclear protein that translocates into cytoplasm following RANKL stimulation [14], therefore, we investigated the effect of glycated-HSA on HMGB1 content in nucleus and cytoplasm after three days of RANKL treatment with or without glycated-HSA. We found cytoplasmic HMGB1 and RAGE had not changed, but nuclear HMGB1 40 and 25 kDa amount was lower in HSA-Glycol treated cells (***Fig. 4***). Cytoplasmic proteins were normalized using GAPDH and nuclear protein using Lamin A/C. HMGB1 is primarily located in the nucleus (0 h), and RANKL stimulation triggers translocation into cytoplasm. HSA-Glycol increased HMGB1 translocation from nucleus to cytoplasm, as nucleus is relatively small compared to cytoplasm, so cytoplasmic HMGB1 was not changed with this additional nuclear HMGB1.

Effect of glycated-HSA on the activation of osteoclastogenic pathways.

As shown in ***Fig. 1-B*** and ***1-D***, HSA-Glycol and HSA-Glycer significantly inhibited osteoclastogenesis, therefore, we investigated their effects on osteoclastogenic pathway activation. In cytoplasm, IκBα is degraded upon RANKL stimulation to activate NFκB, and the activated NFκB then translocate into the nucleus [23-25]. Therefore, we checked the effect of glycated-HSA on cytoplasmic IκBα degradation and nuclear NFκB (p65) accumulation. IκBα was degraded and had the lowest observed amount after 20 minutes of RANKL stimulation, but in the presence of glycated-HSA IκBα, it remained almost same amount (***Fig. 5-A***). NFκB (p65) translocation into the nucleus was also suppressed by glycated-HSA. This data suggested that glycated-HSA downregulated RANKL-induced NFκB (p65) activation.

We also investigated the activation of p38MAPK and ERK using whole cell lysate. Phosphorylation of p38MAPK was not significantly changed, but ERK phosphorylation was significantly induced after 30 and 60 min of treatment with glycated-HSA (***Fig. 5-B***).

Effect of glycated-HSA on siRAGE treated RAW264.7 cell pathway activation

Glycated-HSA inhibited NFκB activation and induced ERK activation, therefore, we investigated whether this is done by RAGE or not. To verify this, we transfected RAW

264.7 cells using siRAGE to downregulate RAGE expression (***Fig. 6-A***). SiRAGE significantly downregulated RAGE expression compared to both no transfection and negative control. Then, siRAGE was used to transfect the RAW264.7 cells, and then, the cells were treated with RANKL with or without glycated-HSA for 30 minutes. Whole cell lysate was prepared and used for western blot analyses to detect pERK, IκBα p-p65, p65, GAPDH protein expression. Compared to ***Fig. 5***, in siRAGE treated cells, pERK was significantly downregulated in the presence of glycated-HSA and IκBα, p-p65 was not altered by glycated-HSA (***Fig. 6-B***), showing that RAGE plays a crucial role on excess ERK activation and the inhibition of IκBα degradation by glycated-HSA.

Effect of glycated-HSA and NFκB inhibitor on NFATc1, c-Fos mRNA expression.

NFATc1 is the master transcription factor for osteoclastogenesis. C-Fos is also involved in osteoclastogenesis [21, 26-29]. Therefore, we investigated whether glycated-HSA have any effects on NFATc1 and c-Fos expression. In our previous experiments, we found that NFATc1 expression was highest following six hours of RANKL treatment [19]. Glycated-HSA significantly inhibited NFκB pathways (***Fig. 5-A***). Therefore, we observed the effects of glycated-HSA and NFκB inhibitor on NFATc1 and c-Fos expression after six hours of treatment, along with RANKL. NFκB inhibitor (BAY11-7082, 10 μM) inhibited both NFATc1 and c-Fos in RANKL treated cells. Also, HSA-Glycol and HSA-Glycer significantly inhibited NFATc1 and c-Fos mRNA expression at doses of 150 and 500 μg/mL (***Fig. 7-A***).

Effect of glycated-HSA on calcium influx activation.

RANKL stimulation activates calcium influx in macrophage cell to further activate osteoclastogenic pathways [28, 30]. We also investigated whether glycated-HSA inhibited calcium influx. We verified using a Fluo-8 AM kit for up to 500 seconds and found RANKL-stimulation significantly activated calcium influx, heated-HSA along with RANKL also activated immediately, but glycated-HSA inhibited calcium influx in our experimental conditions and the maximum intensity were also significantly lower (***Fig. 7-B***).

Discussion

As glycated protein amounts in serum increased in osteoporotic patients [1, 6-8, 13], we investigated abandoned serum protein HSA glycation and its effects on RANKL-induced osteoclastogenesis in RAW264.7 cells. In this study, we observed that glycated-HSA significantly inhibited RANKL-induced osteoclastogenesis as well as its activation depending on the glycating agents. HSA-Glycol and HSA-Glycer were then used for the remainder of the experiments as glycated protein. RAGE expression was not changed in the mRNA and protein level, but total osteoclastogenesis was reduced, which shows that the inhibitory effect is done after exposure to the RANKL and glycated-HSA. Glycated-HSA inhibited RANKL-induced activation of calcium influx, NFκB, master osteoclastogenic transcription factor NFATc1, c-Fos, and the secretion of nuclear protein HMGB1 that plays a major role in osteoclastogenesis.

We used several glycating agents to prepare glycated-HSA and we observed their effect on RANKL-induced osteoclastogenesis. Glycation of protein creates fluorescence AGEs [17, 18], therefore, we investigated fluorescence AGE formation with our experimental glycating agents. The lowest florescence intensity was shown by HSA-Glu, and the highest by HSA-Glycol (***Fig. 1-A***). In addition, all of the glycating agents that showed inhibitory effects on osteoclastogenesis, showed a significantly higher florescence intensity. A possible reason could be the reaction rate, as glucose and fructose are relatively slow to react compared to the other glycating agents. Based on these data, the fluorescent AGEs play a role in the inhibition of osteoclastogenesis, however, further study will be needed.

AGE-modified BSA was reported to totally inhibit *in vitro* osteoclastogenesis by impairing the commitment of osteoclast progenitors into pre-osteoclast cells through their interaction with specific cell-surface receptors as pre-osteoclast and osteoclast cells expressed several receptors including RAGE [31]. In one study, we have found that glycation varies depending on the protein used and BSA, HSA, and collagen showed different degrees of glycation depending on the glycating agent and protein type [32]. In our present study, glucose, fructose, glycolaldehyde, glyceraldehyde, and glyoxal-derived glycated-HSA showed different degrees of glycation based on the glycating sugar used (***Fig. 1-A***). Glycolaldehyde, glyceraldehyde, and glyoxal-derived glycated-HSA significantly inhibited osteoclastogenic TRAP activity compared to RANKL alone, whereas, heated and glucose, fructose derived glycated-HSA showed no effect (***Fig. 1-B***) without causing cell death (***Fig. 1-C,E***). This shows that the inhibitory effect is glycating agent dependent. In another study we conducted, we also observed that glucose and fructose derived glycated collagen type I and II significantly increased TRAP activity [33]. Together, this concludes that glycation significantly modulate RANKL-induced osteoclastogenesis is based on the protein type and the glycating agents used. To check whether glycated-HSA inhibited osteoclastogenesis or the activation of osteoclast cells, we checked the cell morphology under a microscope and found that glycated-HSA inhibited multinucleated osteoclast cell formation (***Fig. 1-D***) that is osteoclast differentiation is inhibited. When we treated glycated-HSA at a different time point, we found that early treatment of HSA-AGEs did not alter RANKL-induced osteoclastogenesis, while in the presence of glycated-HSA the final two days of a five-day RANKL treatment showed almost the same inhibition of TRAP activity compared to a five-day glycated-HSA treatment (***Fig. 1-F***). Also, in mRNA expression levels, early osteoclastogenic markers did not change by glycated-HSA (***Fig 2-A***), as while later stage markers were inhibited (***Fig. 2-B***). These data indicate that glycated-HSA mediate later stage of osteoclastogenesis, but not early osteoclastogenesis. HSA-AGEs inhibited pre-osteoclast cells from fusing together (***Fig. 1-D***) as there were no changes in early osteoclastogenic marker gene expression suggested that early osteoclastogenesis was unaffected by HSA-AGEs.

Non-histone nuclear protein HMGB1, upon activation by RANKL, is released by macrophages into the extracellular environment and then bind with RAGE and plays a crucial role in both *in vivo* and *in vitro* osteoclastogenesis by regulating actin cytoskeleton reorganization [14]. In our study, cellular HMGB1 of RANKL-induced cells was not changed upon time, but secretion was induced time dependently,

and reached highest after three days of treatment. We had to renew culture media after three days, so four-day media did not show HMGB1 (***Fig. 3-A***). To observe HMGB1 secretion, we have chosen a three day time frame. We found three bands of HMGB1, so we confirmed all of the bands were HMGB1 by siHMGB1 experiments as siHMGB1 downregulated all of the three bands in media, but not in cell lysate (***Fig. 3-B***). RAGE expression was induced by RANKL treatment and was highest between 18 hours and three days, then declined, which shows that RAGE plays an important role in osteoclastogenesis (***Fig. 3-A***).

Next, we observed the effect of heated and glycated-HSA on HMGB1 and RAGE expression by the cell and HMGB1 secretion into media. We observed that HMGB1 and RAGE expression were not changed in cell lysate by glycated-HSA (***Fig. 3-C***), but HMGB1 secretion declines (***Fig. 3-D***). Therefore, we investigated whether glycated-HSA inhibition of HMGB1 secretion is dose dependent. We used glycated-HSA 150 and 500 μg/mL and found their ability to decrease HMGB1 secretion was the same, and not dose dependent. It reached the level of no-RANKL treatment (***Fig. 3-E***). As HMGB1 is a multifunctional nuclear protein, we found it to be secreted in lower amounts into culture media in the absence of RANKL (***Fig. 3-E***), but it did not induce osteoclastogenesis (***Fig. 1-B, D***). Therefore, we can conclude as the HMGB1 secreted upon RANKL-stimulation is playing a crucial role in osteoclastogenesis and glycated-HSA inhibited RANKL-induced HMGB1 secretion, thereby inhibited osteoclastogenesis.

As we found that glycated-HSA inhibits HMGB1 secretion, we observed the effects of glycated-HSA on HMGB1 translocation from nucleus to cytoplasm to see if glycated-HSA inhibited translocation. HMGB1 originally located into the nucleus, and after certain stimulations, it translocates into cytoplasm (***Fig. 4-A*** [0h]). In cytoplasmic fractions, HMGB1 and RAGE was not changed by glycated-HSA (***Fig. 4-A-C***). In nuclear fractions, that HMGB1 was reduced with RANKL treatment shows the role of HMGB1 translocation in osteoclastogenesis. HMGB1 40 kDa and 25 kDa were significantly lowered by HSA-Glycol (***Fig. 4-D,E***). This shows HMGB1 translocation from nucleus to cytoplasm or re-translocation from cytoplasm to nucleus has been inhibited by glycated-HSA and that could be a possible reason for osteoclastogenesis inhibition.

NFκB p38MAPK are known as osteoclastogenic pathways that directly induce osteoclastogenesis [11, 21, 23, 24]. Glycated-HSA significantly inhibited NFκB activation (***Fig. 5-A***), but induced ERK phosphorylation after 30 and 60 minutes of treatment without causing any change in p38MAPK (***Fig. 5-B***). The MEK/ERK pathways were found to suppress osteoclastogenesis in RAW264.7 cells [34]. Under our experimental conditions, glycated-HSA significantly induced ERK activation; it could be responsible for shifting differentiation to proliferation as we found a high level of cell growth (***Fig. 1-C,E***). Many studies show that ERK activation is critical for the fate of signal, it could lead to differentiation as well as proliferation [29, 34-36].

To investigate whether alteration of ERK and NFκB pathway by glycated-HSA is mediated through RAGE or not, we transfected RAW264.7 cells using siRAGE, and then the cells were treated with glycated-HSA in the presence of RANKL. There, we found that glycated-HSA-induced ERK activation was significantly lower in siRAGE transfected cells. Moreover, downregulation of NFκB by glycated-HSA was not observed in siRAGE transfected cells (***Fig. 6-B***). NFATc1 and c-Fos are major osteoclastogenic transcription factor [15, 18, 24]; therefore, we also investigated the effect of glycated-HSA and NFκB inhibitor on NFATc1 and c-Fos expression in RANKL-stimulated RAW264.7 cells. Glycated-HSA inhibited NFκB pathways (***Fig. 5-A***) as well as NFATc1 and c-Fos (***Fig. 7-A***) mRNA expressions. The NFκB inhibitor also inhibited NFATc1 and c-Fos (***Fig. 7-A***) expressions. These data suggest that the effect of HSA-AGEs in differentiation pathways was altered through RAGE.

RANKL-stimulation also induce Ca^{2+}-oscillation, and thereby induce NFATc1 and c-Fos to trigger osteoclastogenesis [28]. Therefore, we also investigated Ca^{2+}-oscillation in our experimental conditions and found glycated-HSA to significantly downregulate (***Fig. 7-B***).

In this study, we observed for the first time that glycation of HSA significantly downregulates osteoclastogenesis based on glycating agents via downregulation of RANKL-stimulated Ca^{2+}-oscillation, NFκB, NFATc1, c-Fos activation and HMGB1 secretions.

Conclusion

Depending on the glycating agents and fluorescence AGE production, glycated-HSA significantly inhibited RANKL-induced osteoclastogenesis by downregulating RANKL-signaling in RAW264.7 cells.

Acknowledgements

This work was partially supported by the Japanese Council for Science, Technology and Innovation, SIP (Project ID 14533567), "Technologies for creating next-generation agriculture, forestry and fisheries" (funding agency: Bio-oriented Technology Research Advancement Institution, NARO).

Conflict of interest

The authors claim no conflict of interest in this study.

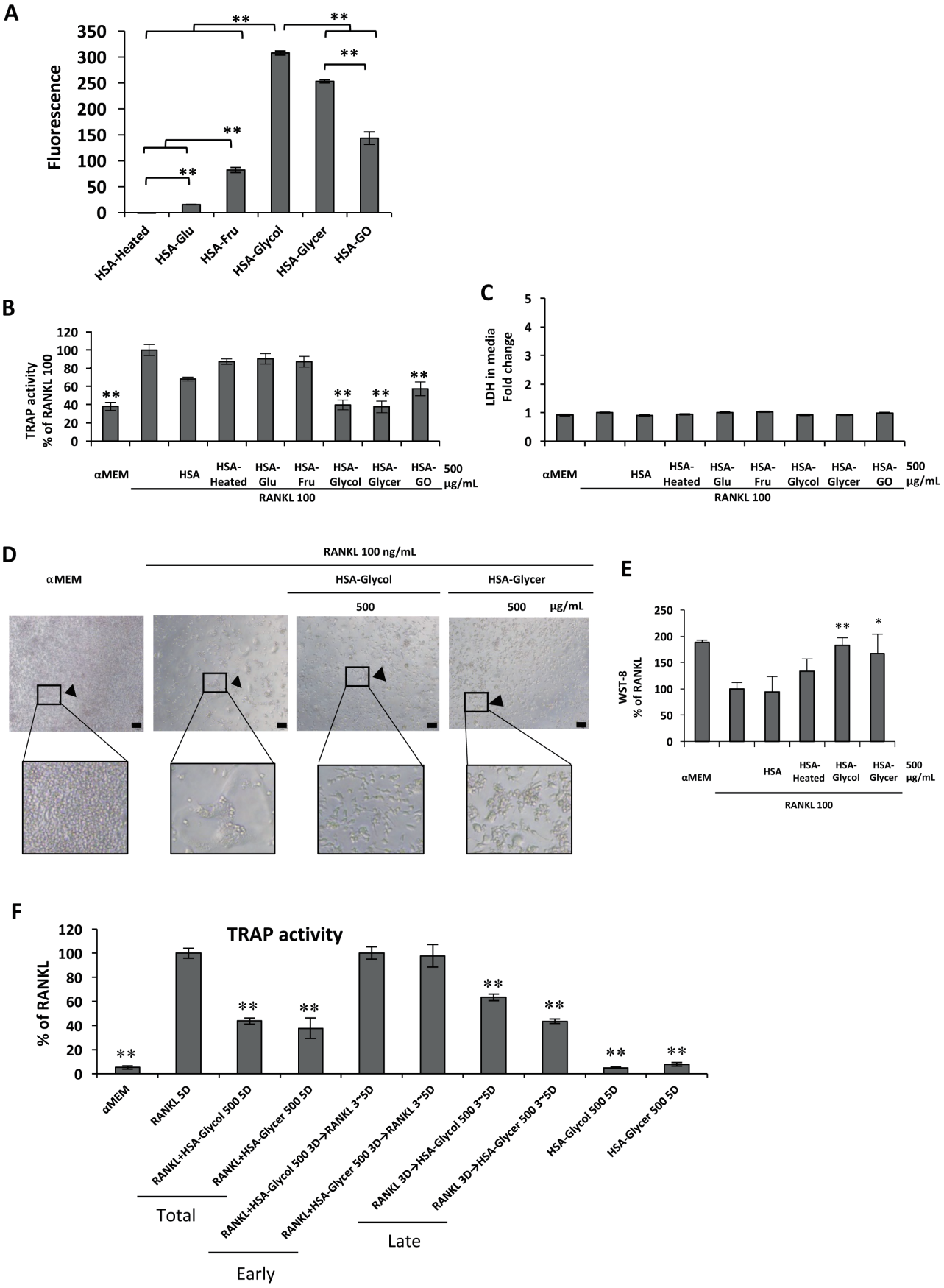

Fig. 1. **Effect of glycated-HSA on RAW264.7 cell osteoclastic differentiation.**

A. Fluorescence intensity of glycated-HSA 150 μg/mL. Values are means ± SEM (n = 3, each group), Tukey-Kramer test, $^{**}p < 0.01$, $^{*}p < 0.05$. **B.** RAW264.7 cells were treated with HSA (native, heated, glycated) in the presence of RANKL for 5 days, and then TRAP activity was measured. **C.** LDH secreted into media by the experimental cells. **D.** Morphology of the HSA-Glycol and HSA-Glycer treated osteoclast cells. The bar represents 100 μm. **E.** WST-8 assay was performed by the experimental cells. **F.** TRAP activity at Day 5 treated with RANKL and HSA-AGEs for 5 days (Total), day 0 to 3 (Early) and Day 3 to 5 (Late). A five-day treatment of HSA-AGEs in the absence of RANKL was also performed. Values are means ± SEM (n = 6, each group), Tukey-Kramer test, $^{**}p < 0.01$, $^{*}p < 0.05$.

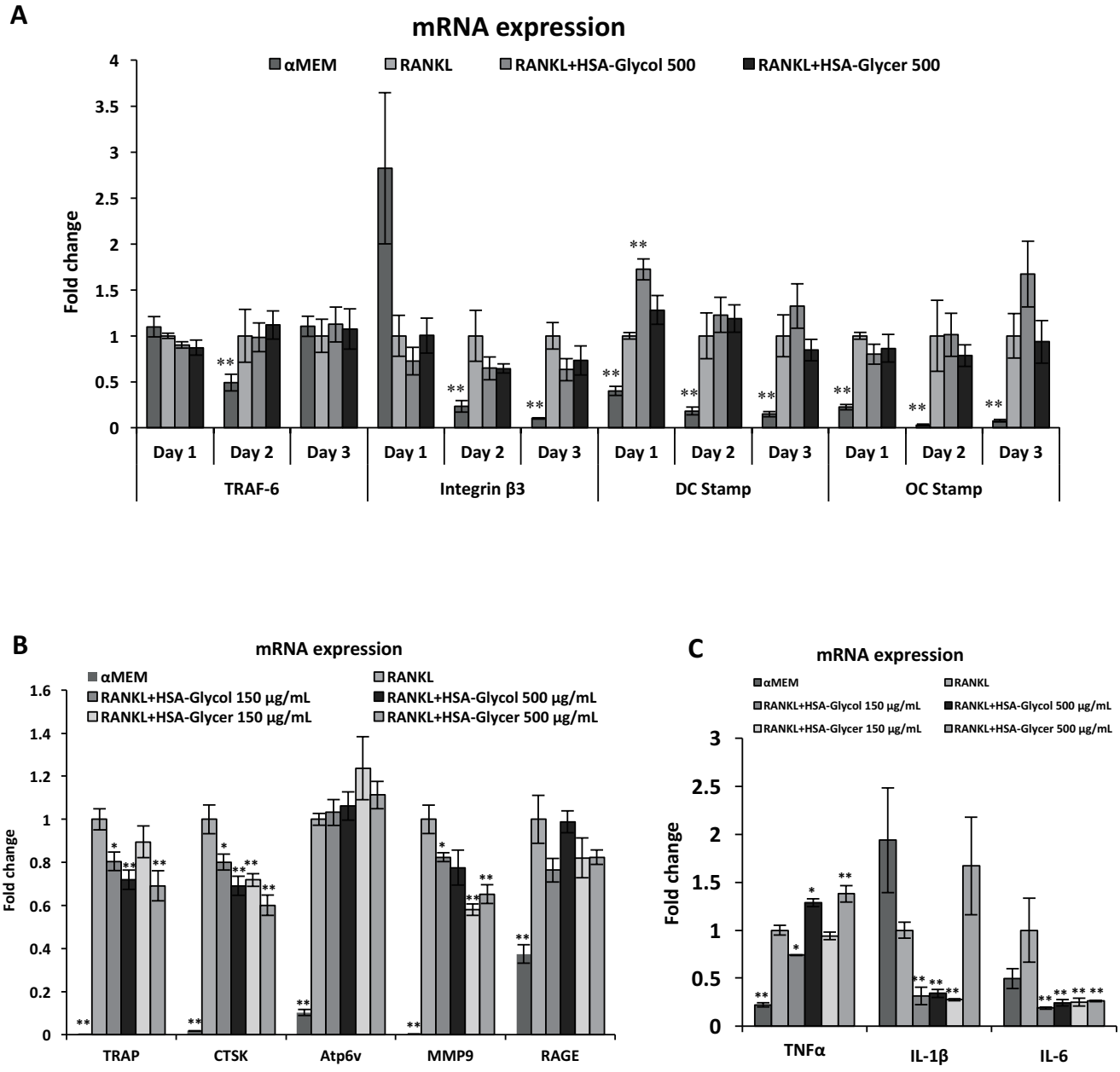

Fig. 2. **Effect of glycated-HSA on osteoclastic and inflammatory mRNA expressions in RAW264.7 cells.**

A. Early osteoclastogenic and fusion related markers such as TRAF-6, Integrin β3, DC stamp, OC stamp mRNA expressions after 1, 2 and 3 days, Values are means ± SEM (n = 4, each group), Tukey-Kramer test, $^{**}p < 0.01$, $^{*}p < 0.05$. **B.** An mRNA expression of osteoclastic maturation marker TRAP, CTSK, Atp6v, MMP9, and RAGE. Values are means ± SEM (n = 4, each group). **C.** An mRNA expression of inflammatory and osteoclastogenic cytokine TNFα, IL-1β, IL-6. Values are means ± SEM (n = 3, each group). TRAF-6, TNF receptor associated factor-6; DC stamp, dendritic cell-specific transmembrane protein; OC stamp, osteoclast stimulatory transmembrane protein; HSA, human serum albumin; RANKL, receptor activator of nuclear factor kappa-B ligand; TRAP, tartrate-resistant acid phosphatase; LDH, lactate dehydrogenase; CTSK, cathepsin K; MMP, matrix metallopeptidase; Atp6v, ATPase H^+ transporting V; RAGE, receptor for AGEs; Glu, glucose; Fru, fructose; Glycol, glycolaldehyde; Glycer, glyceraldehyde; GO, glyoxal; TNF, tumor necrosis factor; IL, interleukin; SEM, standard error mean.

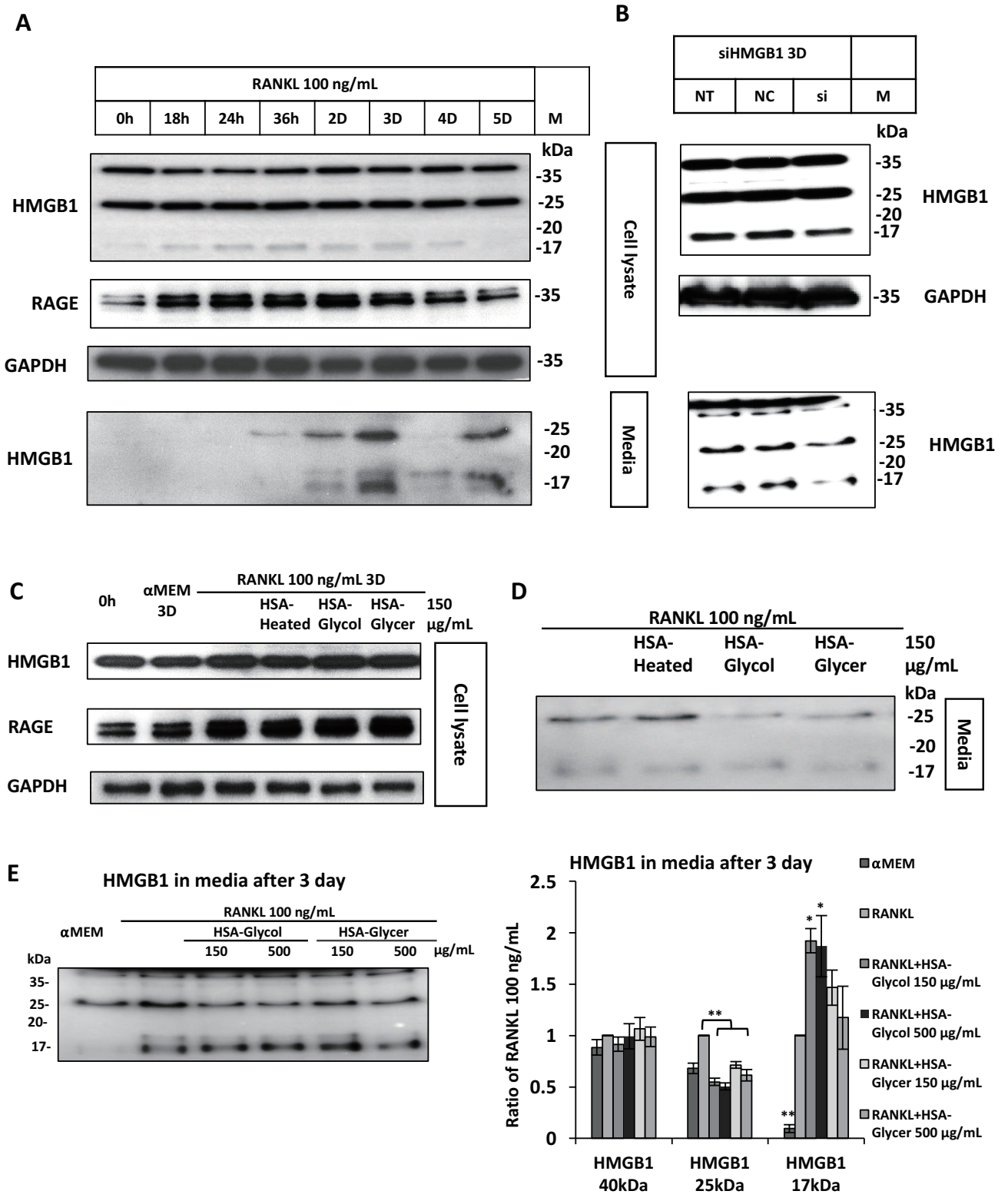

Fig. 3. **HMGB1 and RAGE protein expression by western blot.**

A. RAW264.7 cells were treated with RANKL 100 ng/mL in order to indicate time and expression of HMGB1, RAGE in cell lysate and the secretion of HMGB1 into media. **B.** RAW264.7 cells were transfected using siRNA for HMGB1 for 3 days and then HMGB1 expressions and secretions were recorded. **C.** Effect of heated or glycated-HSA on RANKL-induced RAW264.7 cells after 3 days on HMGB1 and RAGE expression, n = 3. **D.** HMGB1 secretion into media, n = 3. **E.** HMGB1 secretion inhibition by glycated-HSA after 3 days of treatment and ImageJ analysis of band intensity. Values are means ± SEM (n = 11, each group), Tukey-Kramer test, $^{**}p < 0.01$, $^{*}p < 0.05$. HMGB1, high mobility group box 1; RAGE, receptor for AGEs; AGEs, advanced glycation end products; GAPDH, glyceraldehyde 3-phosphate dehydrogenase; RANKL, receptor activator of nuclear factor kappa-B ligand; siRNA, small interfering RNA; RNA, ribonucleic acid; HSA, human serum albumin; NT, no transfection; NC, negative control; si, siHMGB1; SEM, standard error mean.

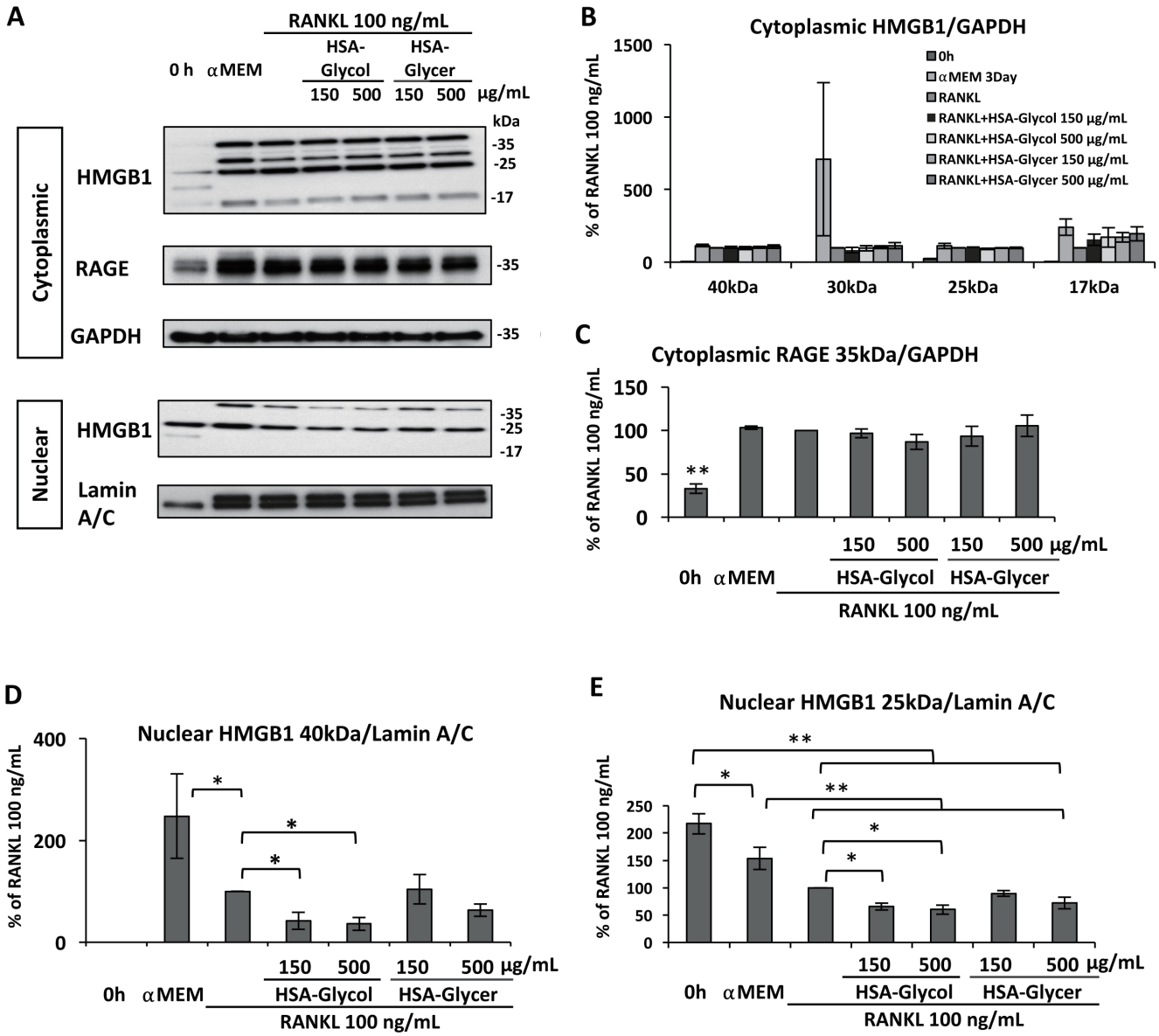

Fig. 4. **Cytoplasmic and nuclear translocation of HMGB1.**

A. RAW264.7 cells were treated with glycated-HSA in the presence of RANKL for 3 days, the cell proteins were fractionated using nuclear and cytoplasmic extraction kits and then checked by western blot for HMGB1, RAGE, GAPDH, Lamin A/C. ImageJ analysis of the band intensity, **B.** Cytoplasmic HMGB1/GAPDH, **C.** Cytoplasmic RAGE/GAPDH, **D.** Nuclear HMGB1 40 kDa/lamin A/C, **E.** Nuclear HMGB1 25 kDa/lamin A/C. Values are means ± SEM (n = 3, each group), Tukey-Kramer test, $^{**}p < 0.01$, $^{*}p < 0.05$. HMGB1, high mobility group box 1; HSA, human serum albumin; RAGE, receptor for AGEs; AGEs, advanced glycation end products; RANKL, receptor activator of nuclear factor kappa-B ligand; GAPDH, glyceraldehyde 3-phosphate dehydrogenase; SEM, standard error mean.

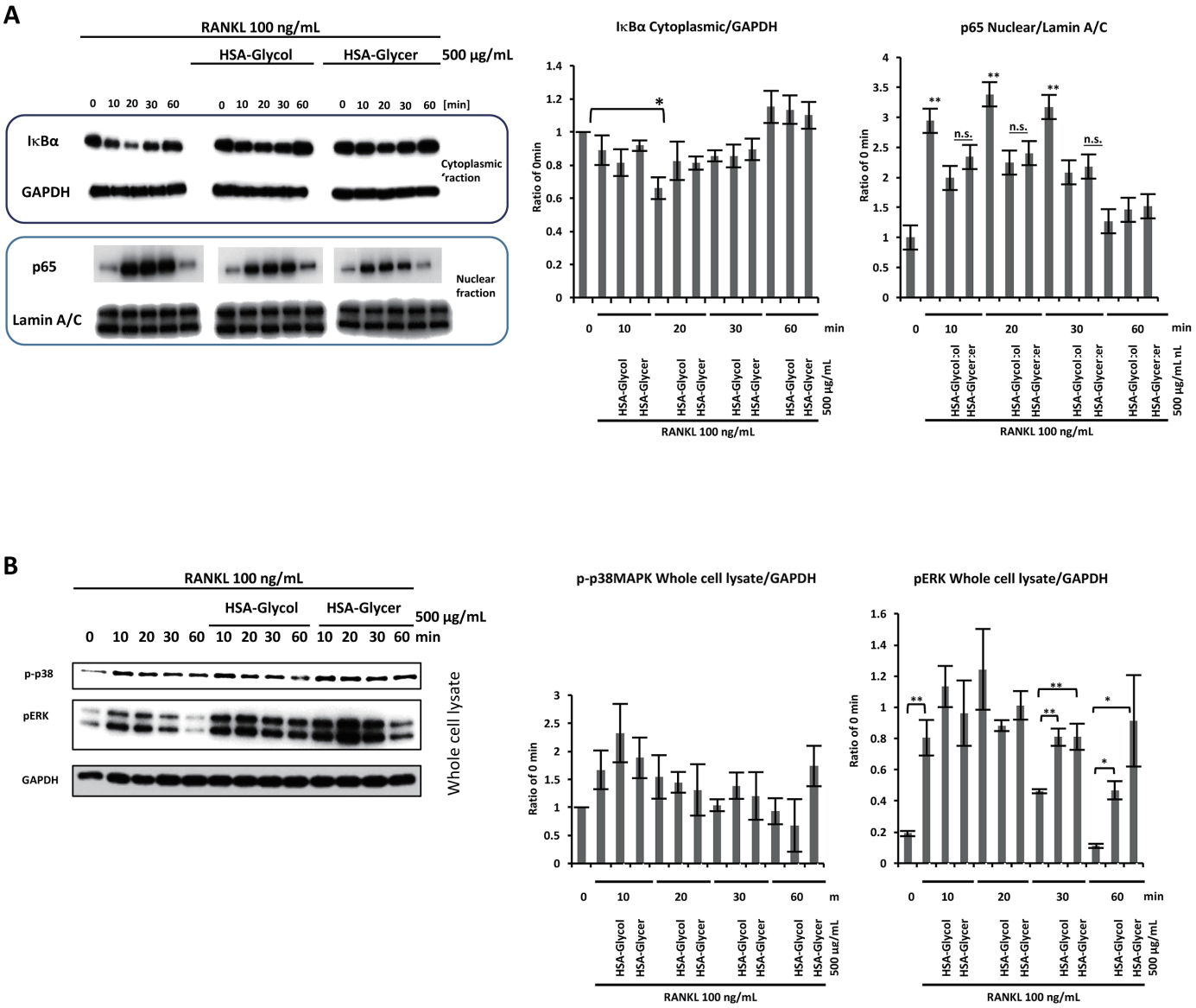

Fig. 5. **Effect of glycated-HSA on osteoclastogenic pathway activation.**

A. NFκB activation by experimental conditions. Cytoplasmic extracts were used for IκBα and nuclear extracts were used for p65 detection by western blot. ImageJ analysis of band intensity. **B.** p38MAPK and pERK activation by experimental conditions in whole cell lysate and ImageJ analysis of band intensity. Values are means ± SEM (n = 3, each group), Tukey-Kramer test, **p < 0.01, *p < 0.05. HSA, human serum albumin; NFκB nuclear factor-κB; IκBα, inhibitor of the NFκB; MAPK, mitogen-activated protein kinases; ERK, extracellular signal-regulated kinases; SEM, standard error mean.

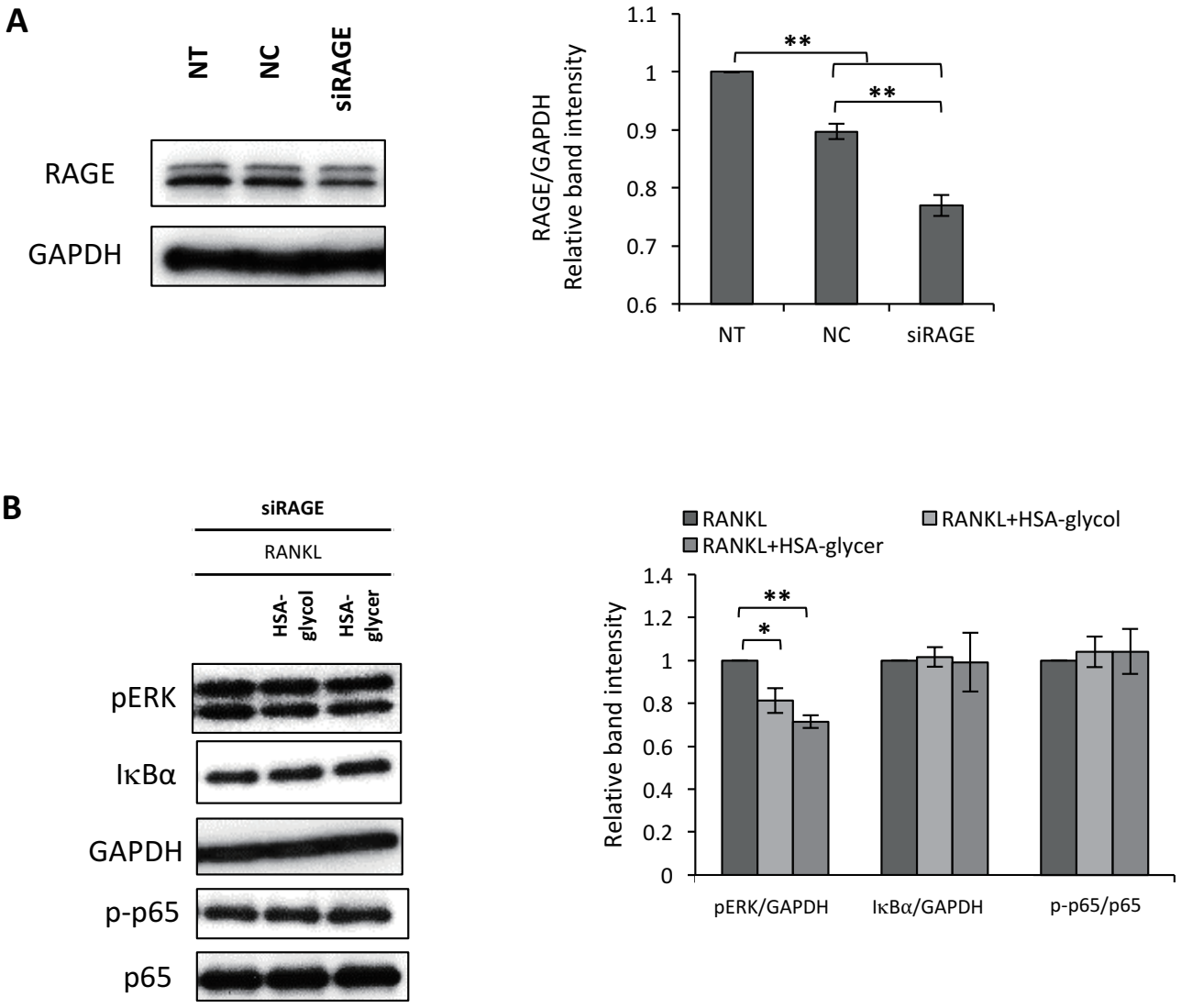

Fig. 6. **Effect of glycated-HSA on siRAGE treated RAW264.7 cell pathway activation.**

A. RAW264.7 cells were transfected using siRAGE to downregulate RAGE expressions. Protein expressions were analyzed by western blot, and band intensities were measured using ImageJ. **B.** RAW264.7 cells were transfected with siRAGE and then treated with RANKL with or without glycated-HSA for 30 min. Following this, cell lysates were used to detect pathway related protein (pERK, IκBα, p-p65, p65, GAPDH) expressions by western blot. Values are means ± SEM (n = 3, each group), Tukey-Kramer test, $^{**}p < 0.01$, $^{*}p < 0.05$. NT, no transfection; NC, negative control; RAGE, receptor for AGEs; AGEs, advanced glycation end products; HSA, human serum albumin; NFκB, nuclear factor-κB; IκBα inhibitor of the NFκB; MAPK, mitogen-activated protein kinases; ERK, extracellular signal-regulated kinases; SEM, standard error mean.

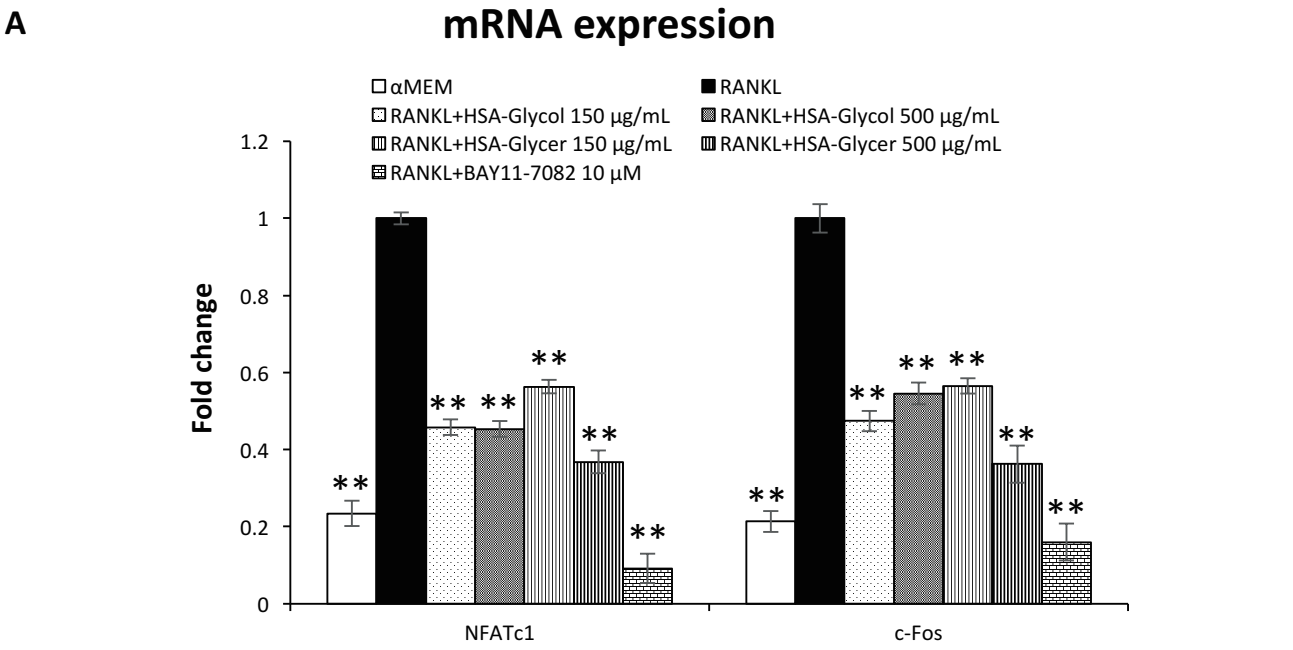

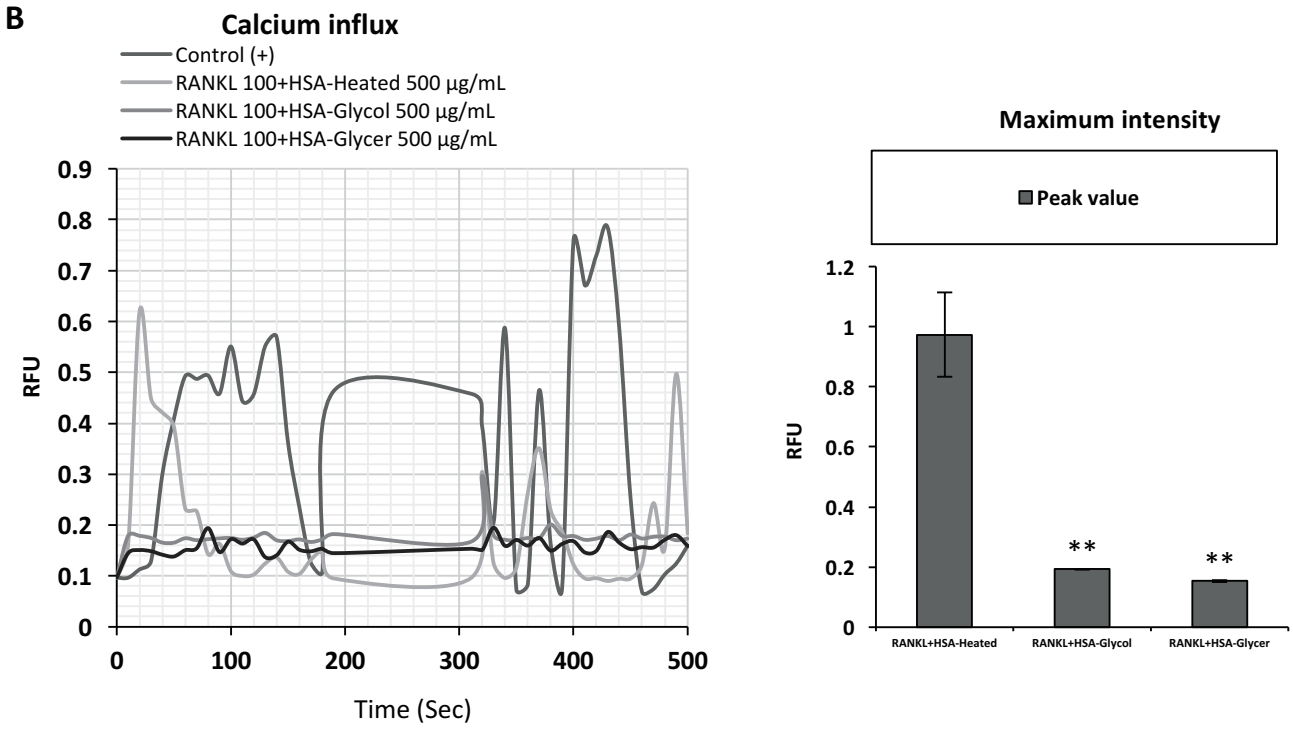

Fig. 7. **Effect of glycated-HSA on osteoclastogenic NFATc1, c-Fos mRNA expression, and calcium influx activation.**

A. RAW264.7 cells were treated with glycated-HSA or BAY11-7082 (NFκB inhibitor) in the presence of RANKL for 6 h, and the mRNA expression of NFATc1 and c-Fos were checked by RT-PCR. Values are means ± SEM (n = 3, each group in two independent experiments), Tukey-Kramer test, **p < 0.01, *p < 0.05. **B.** Calcium influx was checked using a Fluo-8 assay kit for up to 500 seconds. Values are means ± SEM (n = 5, each group), Tukey-Kramer test, **p < 0.01, *p < 0.05. HSA, human serum albumin; NFATc1, nuclear factor of activated T-cells, cytoplasmic 1; RT-PCR, real-time polymerase chain reaction; SEM, standard error mean.

References

1) Hein G, Weiss C, Lehmann G, et al. Advanced glycation end product modification of bone proteins and bone remodelling: Hypothesis and preliminary immunohistochemical findings. Ann Rheum Dis. 2006; 65: 101-104.
2) Lam J, Takeshita S, Barker JE, et al. TNF-α induces osteoclastogenesis by direct stimulation of macrophages exposed to permissive levels of RANK ligand. J Clin Invest. 2000; 106: 1481-1488.
3) Lee SE, Chung WJ, Kwak HB, et al. Tumor necrosis factor-alpha supports the survival of osteoclasts through the activation of Akt and ERK. J Biol Chem. 2001; 276: 49343-49349.
4) Steeve KT, Marc P, Sandrine T, et al. IL-6, RANKL, TNF-alpha/IL-1: Interrelations in bone resorption pathophysiology. Cytokine Growth Factor Rev. 2004; 15: 49-60.
5) Xue J, Rai V, Singer D, et al. Advanced glycation end product recognition by the receptor for AGEs. Structure. 2011; 19: 722-732.
6) Hein G, Wiegand R, Lehmann G, et al. Advanced glycation end-products pentosidine and N-carboxymethyllysine are elevated in serum of patients with osteoporosis. Rheumatology. 2003; 42: 1242-1246.
7) Yang D-H, Chiang T-I, Chang I-C, et al. Increased levels of circulating advanced glycation end-products in menopausal women with osteoporosis. Int J Med Sci. 2014; 11: 453-460.
8) Saito M, Marumo K. New treatment strategy against osteoporosis: Advanced glycation end products as a factor for poor bone quality. Glycative Stress Res. 2015; 2: 1-14.
9) Boyce BF, Rosenberg E, de Papp AE, et al. The osteoclast, bone remodelling and treatment of metabolic bone disease. Eur J Clin Invest. 2012; 42: 1332-1341.
10) Hadjidakis DJ, Androulakis II. Bone remodeling. Ann. N. Y. Acad. Sci. 2006; 1092: 385-396.
11) Soysa NS, Alles N, Aoki K, et al. Osteoclast formation and differentiation: An overview. J Med Dent Sci. 2012; 59: 65-74.
12) Boskey AL, Coleman R. Critical reviews in oral biology &amp: Medicine. J Dent Res. 2010; 89: 1333-1348.
13) Barzilay JI, Bůžková P, Zieman SJ, et al. Circulating levels of carboxy-methyl-lysine (CML) are associated with hip fracture risk: The Cardiovascular Health Study. J Bone Min Res. 2014; 29: 1061-1066.
14) Zhou Z, Han J-Y, Xi C-X, et al. HMGB1 regulates RANKL-induced osteoclastogenesis in a manner dependent on RAGE. J Bone Miner Res. 2008; 23: 1084-1096.
15) Sato K, Yagi M, Umehara H, et al. Establishment of a model for evaluating tumor necrosis factor-α production by cultured RAW264.7 in response to glycation stress. Glycative Stress Res. 2014; 1: 1-7.
16) Mamun-Or-Rashid ANM, Takabe W, Yonei Y. Melatonin has no direct effect on inflammatory gene expression in CML-HSA stimulated RAW264.7 cells. Glycative Stress Res. 2016; 3: 141-151.
17) Hori M, Yagi M, Nomoto K, et al. Experimental models for advanced glycation end product formation using albumin, collagen, elastin, keratin and proteoglycan. Anti-Aging Med. 2012; 9: 125-134.
18) Nomoto K, Yagi M, Hamada U, et al. Identification of advanced glycation endproducts derived fluorescence spectrum *in vitro* and human skin. Anti-Aging Med. 2013; 10: 92-100.
19) Mamun-Or-Rashid ANM, Takabe W, Yagi, et al. RANKL regulates RAW264.7 cell osteoclastogenesis in a manner independent of M-CSF, dependent on FBS, media content and cell density. Glycative Stress Res. 2017; 4: 40-52.
20) Park KH, Park B, Yoon DS, et al. Zinc inhibits osteoclast differentiation by suppression of Ca^{2+}-Calcineurin-NFATc1 signaling pathway. Cell Commun Signal. 2013; 11: 74.
21) Ghayor C, Correro RM, Lange K, et al. Inhibition of osteoclast differentiation and bone resorption by N-methylpyrrolidone. J Biol Chem. 2011; 286: 24458-4466.
22) Arriero M del M, Ramis JM, Perelló J, et al. Inositol hexakisphosphate inhibits osteoclastogenesis on RAW 264.7 cells and human primary osteoclasts. PLoS One. 2012; 7: e43187.
23) Abu-Amer Y. NF-κB signaling and bone resorption. Osteoporos Int. 2013; 24: 2377-2386.
24) Boyce BF, Xiu Y, Li J, et al. NF-κB-mediated regulation of osteoclastogenesis. Endocrinol Metab (Seoul, Korea). 2015; 30: 35-44.
25) Yamashita T, Yao Z, Li F, et al. NF-κB p50 and p52 regulate receptor activator of NF-κB ligand (RANKL) and tumor necrosis factor-induced osteoclast precursor differentiation by activating c-Fos and NFATc1. J Biol Chem. 2007; 282: 18245-18253.
26) Song I, Kim JH, Kim K, et al. Regulatory mechanism of NFATc1 in RANKL-induced osteoclast activation. FEBS Lett. 2009; 583: 2435-2440.
27) Park S-H, Kim J-Y, Cheon Y-H, et al. Protocatechuic acid attenuates osteoclastogenesis by downregulating JNK/c-Fos/NFATc1 signaling and prevents inflammatory bone loss in mice. Phyther Res. 2016; 30: 604-612.
28) Gu DR, Hwang J-K, Erkhembaatar M, et al. Inhibitory effect of *Chrysanthemum zawadskii* Herbich var. *latilobum kitamura* extract on RANKL-induced osteoclast differentiation. Evid Based Complement Alternat Med. 2013; 2013: 509482.
29) Balmanno K, Cook SJ. Sustained MAP kinase activation is required for the expression of cyclin D1, p21Cip1 and a subset of AP-1 proteins in CCL39 cells. Oncogene. 1999; 18: 3085-3097.
30) Kanagawa H, Masuyama R, Morita M, et al. Methotrexate inhibits osteoclastogenesis by decreasing RANKL-induced calcium influx into osteoclast progenitors. J Bone Miner Metab. 2016; 34: 526-531.
31) Valcourt U, Merle B, Gineyts E, et al. Non-enzymatic glycation of bone collagen modifies osteoclastic activity and differentiation. J Biol Chem. 2007; 282: 5691-5703.

32) Moniruzzaman M, Parengkuan L, Yagi M, et al. Effect of proteins, sugars and extraction methods on the anti-glycation activity of spices. Glycative Stress Res. 2015; 2: 129-139.
33) Mamun-Or-Rashid ANM, Takabe W, Yagi M, et al. Glycated-proteins modulate RANKL-induced osteoclastogenesis in RAW264.7 cells. Glycative Stress Res. 2017; 4: 232-239.
34) Hotokezaka H, Sakai E, Kanaoka K, et al. U0126 and PD98059, specific inhibitors of MEK, accelerate differentiation of RAW264.7 cells into osteoclast-like cells. J Biol Chem. 2002; 277: 47366-47372.
35) New L, Li Y, Ge B, et al. SB203580 promote EGF-stimulated early morphological differentiation in PC12 cell through activating ERK pathway. J Cell Biochem. 2001; 83, 585-596.
36) Weber JD, Raben DM, Phillips PJ, et al. Sustained activation of extracellular-signal-regulated kinase 1 (ERK1) is required for the continued expression of cyclin D1 in G1 phase. Biochem J. 1997; 326: 61-68.